Analysis of the Long-Term Performance Degradation of Crystalline Silicon Photovoltaic Modules in Tropical Climates

Wei Luo, Yong Sheng Khoo, Peter Hacke, Dirk Jordan, Lu Zhao, Seeram Ramakrishna, Armin G. Aberle, and Thomas Reindl

***Abstract*—The long-term performance degradation of five different types of commercial crystalline silicon (c-Si) photovoltaic (PV) modules (one sample for each type) in the tropics, or more specifically the tropical rainforest climate "Af" by the Köppen climate classification (Singapore), is investigated over a period of seven years, based on outdoor *I–V* measurements at 10-s intervals. The degradation rates of these c-Si PV modules, based on the temperature-corrected performance ratio, range from –0.03 to –0.47%/year, which satisfy the products' performance warranty. Further analysis of the short-circuit current (I_{sc}), open-circuit voltage, and fill factor for these modules shows that the performance degradation is mainly attributed to the I_{sc} loss. The possible causes of the module performance deterioration are also discussed.**

***Index Terms*—Crystalline silicon (c-Si) modules, degradation modes, degradation rates, long-term module performance in the tropics, photovoltaics (PVs).**

I. Introduction

THE long-term photovoltaic (PV) module performance is a crucial factor for the energy yield and economics of PV systems/installations worldwide. With a more reliable and durable design, PV modules produce more electricity over their operating lifetime, which directly translates into a lower levelized cost of electricity and carbon emissions of PV generation [1]. Over the past few decades, PV module manufacturers have worked diligently on improving the long-term reliability of their products, whereby the performance warranty has increased from 20 to 25 years or more. Furthermore, the warrantied power after 25-year life has increased from 80% to up to 92% [2], [3]. However, despite the continuous efforts, PV modules are susceptible to various types of degradation in the field, such as corrosion of solder joints [4], discoloration of encapsulants [5], adhesion loss between encapsulants and other layers [6], hotspots [7], [8], and potential-induced degradation (PID) [9]–[13]. The degradation modes and rates are both climate- and technology-dependent [14], [15]. Accelerated stress testing procedures are being developed to identify design, material, and process flaws that could cause early-stage failures. However, ensuring the performance of PV modules over 25 years in the field is extremely challenging.

With the rapid growth of the PV deployment, understanding the long-term performance of PV modules becomes highly valuable. Knowledge of module performance degradation rates is important for forecasting the energy yield from PV power plants over their operational lifetime. In addition, identifying degradation modes and possible root causes provides insights and guidance for future research and product developments. Several studies have investigated that the outdoor performance degradation of various PV module technologies at different locations [16]–[21], but information on the long-term reliability of PV modules installed in the tropics is limited. Furthermore, previous studies of module performance degradation in the tropics are mostly based on data collected for less than five years [22]–[24]. The present study investigates the long-term stability of five different types of crystalline silicon (c-Si) PV modules (one sample for each type), which were monitored over a period of seven years from September 2010 to August 2017 in Singapore (the tropical rainforest climate "Af" by the Köppen climate classification [25]). We focus on the performance degradation rates of these modules, based on outdoor *I–V* measurements at 10-s intervals. The degradation modes and root causes of the performance loss are also studied and discussed.

II. Experimental Design

The PV modules were installed in August 2010 on the rooftop of a building at the National University of Singapore (NUS) campus (1.301897°N, 103.77245°E), as shown in Fig. 1. Five

Manuscript received July 26, 2018; revised September 15, 2018; accepted October 9, 2018. The work at the Solar Energy Research Institute of Singapore was supported by the National University of Singapore and Singapore's National Research Foundation through the Singapore Economic Development Board. The work at the National Renewable Energy Laboratory was supported by the U.S. Department of Energy under Contract DE-AC36-08GO28308 with Alliance for Sustainable Energy, LLC, the Manager and Operator of the National Renewable Energy Laboratory. *(Corresponding author: Thomas Reindl.)*

W. Luo and S. Ramakrishna are with the Solar Energy Research Institute of Singapore, Singapore 117574, and also with the Department of Mechanical Engineering, National University of Singapore, Singapore 117575 (e-mail: serlw@nus.edu.sg; seeram@nus.edu.sg).

Y. S. Khoo, L. Zhao, and T. Reindl are with the Solar Energy Research Institute of Singapore, Singapore 117574 (e-mail: yongshengkhoo@nus.edu.sg; zhaoluu@gmail.com; thomas.reindl@nus.edu.sg).

P. Hacke and D. Jordan are with the National Renewable Energy Laboratory, Golden, CO 80410 USA (e-mail: peter.hacke@nrel.gov; Dirk.Jordan@nrel.gov).

A. G. Aberle is with the Solar Energy Research Institute of Singapore, Singapore 117574, and also with the Department of Electrical and Computing Engineering, National University of Singapore, Singapore 117583 (e-mail: armin.aberle@nus.edu.sg).

Color versions of one or more of the figures in this paper are available online at http://ieeexplore.ieee.org.

Digital Object Identifier 10.1109/JPHOTOV.2018.2877007

Fig. 1. Test setup for monitoring the long-term performance of PV modules on the rooftop of a building at the NUS campus.

types of commercially available c-Si PV modules (one sample for each type) were monitored and analyzed. The information of the modules is summarized in Table I; some specifications are deliberately withheld to keep the specific module models anonymous. They have been mounted on open racks with more than 1 m above the ground level to ensure good ventilation; they have been facing true south and were mounted slightly higher than the latitude tilt at 10° to allow sufficient self-cleaning. Each module has been individually monitored using high-precision maximum power point (MPP) trackers. *I–V* characteristics were measured at 10-s intervals, and the modules were operating at their MPPs between the *I–V* measurements to simulate the real-world operating conditions. The in-plane irradiance and module temperature (measured on the back of the modules) were also measured and logged every 10 s. No external high-voltage bias was applied to the modules; therefore, PID is not considered in this study. Most of the light-induced degradation (LID) had already occurred prior to the outdoor *I–V* measurements due to pre-conditioning. Both, the MPP trackers and the irradiance sensors were calibrated every two years according to the manufacturers' requirements. The irradiance sensors were cleaned once every week, whereas the modules were intentionally not cleaned; therefore, soiling losses are included in the overall degradation. Weekly checking of the modules was conducted to ensure that there were no substantial particles on the module surfaces and the irradiance sensor (e.g., bird droppings), and that there was a good adhesion of the temperature sensors to the back of the modules.

TABLE I
SUMMARY OF THE INFORMATION ON THE INVESTIGATED MODULES

Module type	Module construction	Frame	Nominal power (W_p)
- multicrystalline silicon (mult'-	glass/backsheet	Yes	230
-	/backsheet	Yes	180
- monocrystalline Si (mon -	glass/glass	No	170
-	/backsheet	Yes	210
- bac - (IBC)	glass/backsheet	Yes	95

III. Analytical Methods

A. Data Filtering

Two filters are applied to remove the non-representative data and outliers. A clearsky index (csi) filter of 30% width (i.e., $0.7 \leq \text{csi} \leq 1.3$) is used to eliminate data collected during extremely cloudy conditions, which can cause noticeable errors to *I–V* measurements and produce low-quality data [26]. The csi is calculated by taking the ratio of the measured in-plane irradiance to the modeled clearsky in-plane irradiance [26]. The modeled clearsky in-plane irradiance is determined using the modeling tools in PVLIB [27], based on site information such as longitude, latitude, and altitude, as described in [26]. The second filter is for irradiance thresholds [28]. A low irradiance threshold (G_{low}) of 200 W/m^2 and a high irradiance threshold (G_{high}) of 1200 W/m^2 are imposed. The low irradiance condition is mainly to remove nighttime data, non-uniform irradiance, and unstable scenarios [26], [28]. On the other hand, high irradiances exceeding 1200 W/m^2 are mainly due to cloud reflections, since the modeled clearsky irradiance in Singapore is generally below 1000 W/m^2 [22], [29]. More than 30% of the data are retained after the two filtering steps.

B. Performance Metrics

Temperature-corrected performance ratio ($\text{PR}_{\text{corrected}}$), defined by (1), is used for the long-term module performance degradation analysis [26]. $\text{PR}_{\text{corrected}}$ is calculated at each timestamp and then aggregated into daily $\text{PR}_{\text{corrected}}$ based on an insolation-weighted average

$$\text{PR}_{\text{corrected}} = \frac{P_{\text{MPP}}}{P_{\text{STC,rated}} * \frac{G_{\text{in-plane}}}{G_{\text{ref}}} * [1 + \gamma * (T_{\text{module}} - T_{\text{ref}})]} \quad (1)$$

where P_{MPP} is the measured module power at MPP, $P_{\text{STC,rated}}$ is the rated module power at standard testing conditions (STC), $G_{\text{in-plane}}$ is the measured in-plane irradiance, G_{ref} is the reference irradiance of 1000 W/m^2, γ is the maximum power temperature coefficient and the value is based on the manufacturer's specifications, T_{module} is the measured module temperature, and T_{ref} is the reference temperature of 25 °C.

To identify possible causes of performance degradation, the degradation trends of short-circuit current (I_{sc}), open-circuit voltage (V_{oc}), and fill factor (FF) are also analyzed. I_{sc}, V_{oc}, and FF are translated into the reference conditions (STC) by (2)–(5) [30]–[32] and then aggregated into daily values. V_{oc} is not corrected for irradiance, which has only a small effect on the absolute values and a negligible effect on the degradation rate [30]

$$I_{\text{sc,ref}} = \frac{G_{\text{ref}}}{G_{\text{in-plane}}} * \frac{I_{\text{sc}}}{1 + \alpha^* (T_{\text{module}} - T_{\text{ref}})} \quad (2)$$

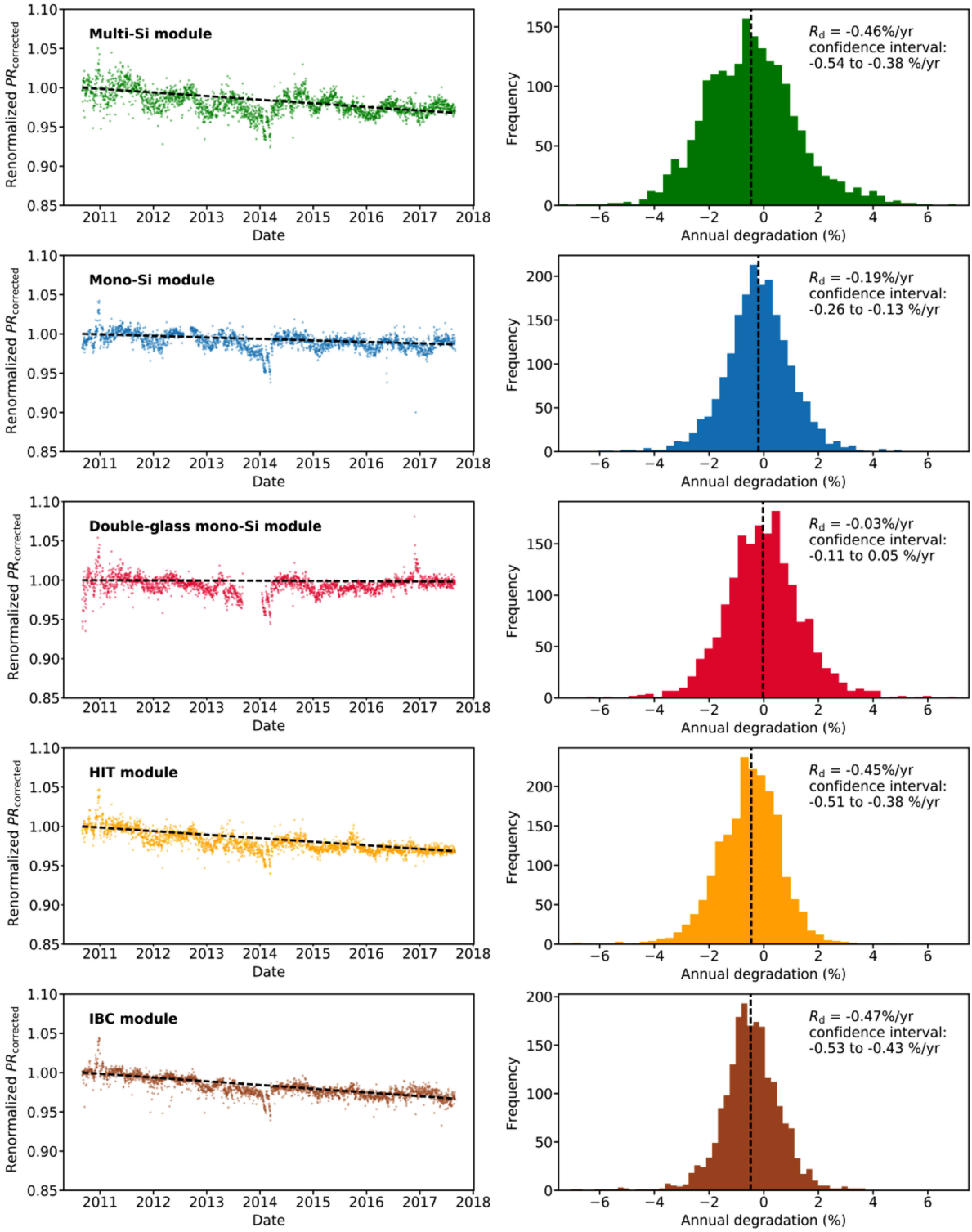

Fig. 2. Measured performance degradation of various c-Si modules in Singapore over a period of seven years. The left column is the evolution of the daily renormalized $\mathrm{PR}_{\mathrm{corrected}}$, and the right column is the corresponding histogram of the annual degradation rage (R_d) based on the YOY analysis. The dash lines on the left-side figures represent the degradation trends based on the YOY analysis, where the vertical dash lines on the right-side figures represent the median of the R_d distribution. The data outage for the double-glass mono-Si module from early September 2013 to middle January 2014 was due to equipment maintenance. PR values are renormalized for plotting. The 95% confidence interval for R_d is calculated by the bootstrap method.

$$V_{\mathrm{oc,ref}} = \frac{V_{\mathrm{oc}}}{1+\beta*(T_{\mathrm{module}}-T_{\mathrm{ref}})} \tag{3}$$

$$P_{\mathrm{MPP,ref}} = \frac{G_{\mathrm{ref}}}{G_{\mathrm{in-plane}}} * \frac{P_{\mathrm{MPP}}}{1+\gamma^{*}(T_{\mathrm{module}}-T_{\mathrm{ref}})} \tag{4}$$

$$\mathrm{FF}_{\mathrm{ref}} = \frac{P_{\mathrm{MPP,ref}}}{{I_{\mathrm{sc,ref}}}^{*}\, V_{\mathrm{oc,ref}}} \tag{5}$$

where $I_{\mathrm{sc,ref}}$, $V_{\mathrm{oc,ref}}$, $P_{\mathrm{MPP,ref}}$, and $\mathrm{FF}_{\mathrm{ref}}$ are the corrected values at the reference conditions; α, β, and γ are the temperature

coefficients for I_{sc}, V_{oc}, and P_{MPP}, respectively, which are based on the manufacturers' specifications.

C. Degradation Analysis

The year-to-year (YOY) methodology is used to analyze the annual degradation rates of $PR_{corrected}$, I_{sc}, V_{oc}, and FF. This method was proposed by Hasselbrink *et al.* [33], with which they investigated the performance loss of 266 PV systems consisting of over 80 000 modules and having a total of 3.2 million module-years of operation. It was later validated and further improved by Jordan *et al.* [26], [34], where it was shown that the degradation rates of fielded modules estimated by the YOY method and measured by indoor flashing at STC are in good agreement. In addition, its performance was compared to the conventional standard least squares regression (SLS) approach. The YOY method has a number of advantages over the SLS approach, such as less filtering requirements and less sensitivity to soiling and seasonal variations [26], [34]. However, the YOY method requires multiple years of data to obtain statistical significance [34]. As this study consists of seven years of data, the YOY method is an excellent match for our analysis. The YOY method calculates the rate of change between two points at the same time in subsequent years, which in this study is the same calendar days. Assembling all the data points produces a statistical distribution, and the annual degradation rate can be determined by the central tendency. In this study, the median of the distribution is used to estimate the degradation rate.

IV. Results and Discussions

A. Module Degradation Rates

Fig. 2 shows the degradation trends of $PR_{corrected}$ of various c-Si modules installed in Singapore. The double-glass mono-Si module exhibited the lowest performance degradation of –0.03%/year, while the conventional mono-Si module showed a slightly higher performance degradation with a degradation rate of –0.19%/year. The multi-Si, heterojunction (HIT), and interdigitated back contact (IBC) modules had similar degradation trends, with a performance decline of –0.46, –0.45, and –0.47%/year, respectively. It is difficult to make fair comparisons between specific c-Si PV module technologies due to the sample size and different module designs, since the types of encapsulants, backsheets, and edge sealants are all important to the long-term module reliability. Nonetheless, it can be concluded that, in general, c-Si PV modules meet the manufacturers' product performance warranty and are suitable for applications in the tropical climate. Twenty-five years of lifetime or more from c-Si modules can be expected, given that proper product quality control measures are taken (e.g., IEC qualification standards).

B. Analysis of Degradation Modes

Analyzing the I_{sc}, V_{oc}, and FF revealed that the cause of degradation for these modules is dominated by a change in I_{sc}, while V_{oc} and FF were relatively less influenced (see Fig. 3). Fig. 4 shows an example of the degradation trends of I_{sc}, V_{oc}, and FF for the multi-Si module. Visual inspections showed no visible changes in appearance to the front encapsulants for all

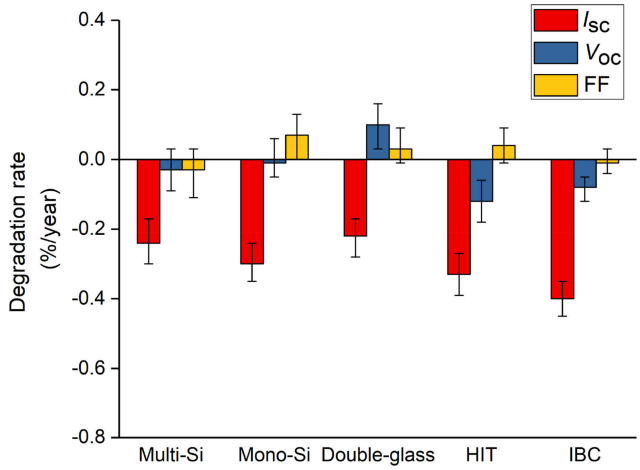

Fig. 3. Annual degradation rates of I_{sc}, V_{oc}, and FF for various c-Si modules in Singapore over a period of seven years based on the YOY analysis. The 95% confidence interval for I_{sc}, V_{oc}, and FF is calculated by the bootstrap method.

c-Si modules, which is usually identified as a cause for current loss in fielded c-Si modules [8]. However, it is possible that the encapsulants (e.g., ethylene-vinyl acetate copolymers) have deteriorated during the long-term outdoor exposure, but the change in the materials' optical properties (e.g., transmittance loss in the ultraviolet range) might not be detectable by the human eye [35], [36]. Osterwald *et al.* also reported that the gradual loss of I_{sc} in c-Si modules could be related to a degradation process of the solar cells' p-n junction [37]. In addition, soiling effects may also have some contribution to the I_{sc} degradation. However, soiling on PV module surfaces is a minor issue in Singapore if the modules are sufficiently tilted ($\sim$10°), as the average number of rainy days is 167 and the mean annual rainfall total is more than 2000 mm [38]. Visual inspections on these modules showed insignificant soiling. On the other hand, discoloration of the cell-side backsheet was observed on the mono-Si module, which reduces the internal reflection and results in a lower current, but this has only a minor impact.

Furthermore, a noticeable increase in V_{oc} ($+0.10$%/year, Fig. 5) was seen for the double-glass mono-Si module, which could suggest recovery from LID to some extent due to the dissociation of boron–oxygen defects [19], [39]. The recovery of LID partially offsets the degradation in the double-glass mono-Si modules, which is one of the reasons why it has the lowest performance loss. In contrast, the HIT module exhibited some loss in V_{oc} (-0.12%/year, Fig. 5), indicating a slight deterioration in the surface passivation quality [19], [40].

C. Impact of the Data Filtering Procedure

The selection of filters is very important to the accuracy of the module performance degradation analysis. Jordan and Kurtz showed that different filtering criteria can lead to different results when evaluating the same dataset [28]. Therefore, different filtering criteria are applied to validate our analysis. First, the width of the csi filter is varied from 5% to 40%, while using the same irradiance thresholds (200 and 1200 W/m^2). Next, the G_{low} is varied from 100 to 600 W/m^2, while keeping the G_{high} at 1200 W/m^2 and the width of the csi filter at 30%. The performance degradation rates of the investigated modules

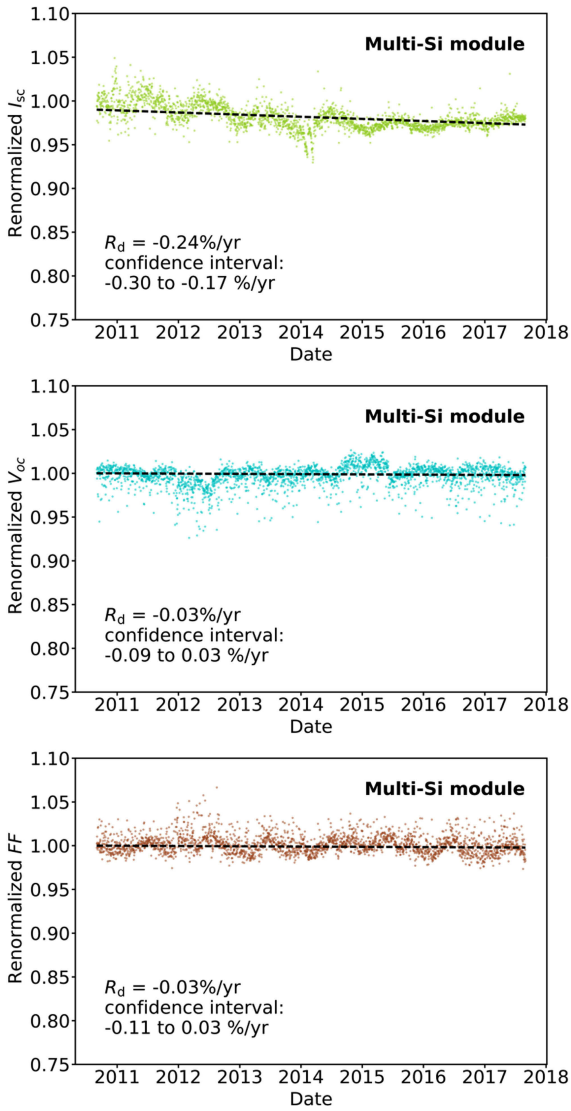

Fig. 4. Degradation trends of I_{sc}, V_{oc}, and FF for the multi-Si module in Singapore over a period of seven years based on the YOY analysis. The dash lines represent the degradation trends I_{sc}, V_{oc}, and FF values are renormalized for plotting. The 95% confidence interval for I_{sc}, V_{oc}, and FF is calculated by the bootstrap method.

at different scenarios are summarized in Fig. 6. The data points shown in black represent the results when the width of the csi filter is 30%, with a G_{low} of 200 W/m^2 and a G_{high} of 1200 W/m^2. As shown in Fig. 6, the performance degradation rates of various modules vary with the applied filtering criteria. In general, a more stringent csi filter yields slightly slower degradation for the multi-Si, mono-Si, double-glass mono-Si, and HIT modules, but the opposite is true for the IBC module. Compared with the csi filter, the low irradiance threshold shows more impact on the performance degradation rates, where the most change is seen for the multi-Si module. Increasing the G_{low} generally leads to a larger degradation rate. However, the variations due to the filtering (including both the csi and irradiance filters) are well within the 95% confidence interval. Therefore, it can be concluded that the filters used in this study do not bias the findings and are justified.

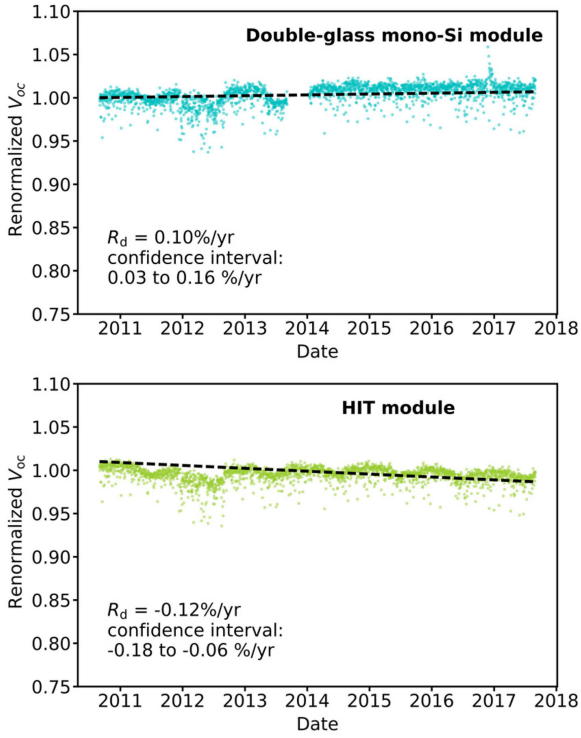

Fig. 5. Degradation trends of V_{oc} for the double-glass mono-Si (top) and HIT module (bottom) in Singapore over a period of seven years based on the YOY analysis. The dash lines represent the degradation trends. V_{oc} values are renormalized for plotting. The 95% confidence interval for V_{oc} is calculated by the bootstrap method.

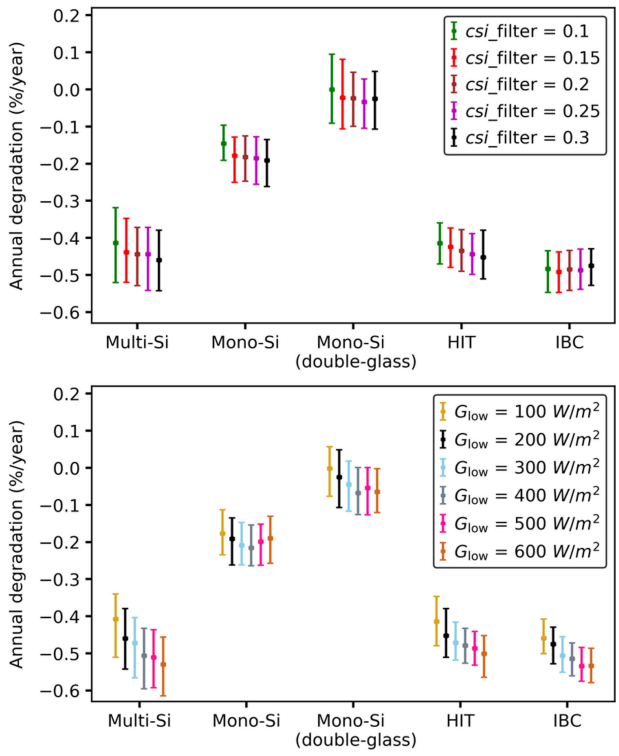

Fig. 6. Summary of the annual degradation rates of various c-Si modules after using different filtering criteria. The top diagram shows the R_d when the csi filter is varied, and the bottom diagram shows the R_d when the G_{low} is varied. The 95% confidence interval for R_d is calculated by the bootstrap method.

V. Conclusion

This study investigated the long-term performance degradation of five types of commercial c-Si PV modules in tropical Singapore over a period of seven years, based on outdoor *I–V* measurements using high-precision MPP trackers. The annual performance degradation rates of these c-Si modules, based on $PR_{corrected}$, range from –0.03 to –0.47%/year. While it is difficult to differentiate between specific c-Si module technologies, it can be concluded that the products meet the manufacturers' long-term performance warranty (PID and LID are not considered) and are suitable for applications in the tropical climate. The cause of degradation for these modules was shown to be dominated by a loss in the I_{sc}, which could be due to changes in the optical transmittance of the encapsulants, p-n junction degradation, and/or soiling effects. Moreover, the double-glass mono-Si module exhibited a noticeable increase in V_{oc}, which indicates a recovery from LID. On the other hand, the HIT module suffered a substantial loss in V_{oc}, suggesting changes in the surface passivation quality.

References

[1] W. Luo *et al.*, "A comparative life-cycle assessment of photovoltaic electricity generation in Singapore by multicrystalline silicon technologies," *Sol. Energy Mater. Sol. Cells*, vol. 174, pp. 157–162, 2018.

[2] LG, Feb. 22, 2018. [Online]. Available: http://www.lg.com/global/business/solar/neon-r

[3] SUNPOWER, Feb. 22, 2018. [Online]. Available: https://us.sunpower.com/home-solar/solar-cell-technology-solutions/

[4] M. A. Quintana, D. L. King, T. J. McMahon, and C. R. Osterwald, "Commonly observed degradation in field-aged photovoltaic modules," in *Proc. 29th IEEE Photovolt. Spec. Conf.*, New Orleans, LA, USA, 2002, pp. 1436–1439.

[5] F. J. Pern, "Ethylene-vinyl acetate (EVA) encapsulants for photovoltaic modules: Degradation and discoloration mechanisms and formulation modifications for improved photostability," *Die Angewandte Makromolekulare Chemie*, vol. 252, no. 1, pp. 195–216, 1997.

[6] J. H. Wohlgemuth *et al.*, "Assessing the causes of encapsulant delamination in PV modules," in *Proc. 43rd IEEE Photovolt. Spec. Conf.*, Portland, OR, USA, 2016, pp. 0248–0254.

[7] J. Qian, A. Thomson, A. Blakers, and M. Ernst, "Comparison of half-cell and full-cell module hotspot-induced temperature by simulation," *IEEE J. Photovolt.*, vol. 8, no. 3, pp. 834–839, May 2018.

[8] D. C. Jordan, T. J. Silverman, J. H. Wohlgemuth, S. R. Kurtz, and K. T. VanSant, "Photovoltaic failure and degradation modes," *Prog. Photovolt.: Res. Appl.*, vol. 25, no. 4, pp. 318–326, 2017.

[9] W. Luo *et al.*, "In-Situ characterization of potential-induced degradation in crystalline silicon photovoltaic modules through dark I–V measurements," *IEEE J. Photovolt.*, vol. 7, no. 1, pp. 104–109, Jan. 2017.

[10] W. Luo *et al.*, "Investigation of potential-induced degradation in n-PERT bifacial silicon photovoltaic modules with a glass/glass structure," *IEEE J. Photovolt.*, vol. 8, no. 1, pp. 16–22, Jan. 2018.

[11] W. Luo *et al.*, "Investigation of the impact of illumination on the polarization-type potential-induced degradation of crystalline silicon photovoltaic modules," *IEEE J. Photovolt.*, vol. 8, no. 5, pp. 1168–1173, Sep. 2018.

[12] W. Luo *et al.*, "Elucidating potential-induced degradation in bifacial PERC silicon photovoltaic modules," *Prog. Photovolt.: Res. Appl.*, vol. 26, no. 10, pp. 859–867, 2018.

[13] W. Luo *et al.*, "Potential-induced degradation in photovoltaic modules: A critical review," *Energy Environ. Sci.*, vol. 10, no. 1, pp. 43–68, 2017.

[14] D. C. Jordan and S. R. Kurtz, "Photovoltaic degradation rates—An analytical review," *Prog. Photovolt.: Res. Appl.*, vol. 21, no. 1, pp. 12–29, 2013.

[15] D. C. Jordan, S. R. Kurtz, K. VanSant, and J. Newmiller, "Compendium of photovoltaic degradation rates," *Prog. Photovolt.: Res. Appl.*, vol. 24, no. 7, pp. 978–989, 2016.

[16] E. D. Dunlop and D. Halton, "The performance of crystalline silicon photovoltaic solar modules after 22 years of continuous outdoor exposure," *Prog. Photovolt.: Res. Appl.*, vol. 14, no. 1, pp. 53–64, 2006.

[17] M. Schweiger, J. Bonilla, W. Herrmann, A. Gerber, and U. Rau, "Performance stability of photovoltaic modules in different climates," *Prog. Photovolt.: Res. Appl.*, vol. 25, no. 12, pp. 968–981, 2017.

[18] A. Pozza and T. Sample, "Crystalline silicon PV module degradation after 20 years of field exposure studied by electrical tests, electroluminescence, and LBIC," *Prog. Photovolt.: Res. Appl.*, vol. 24, no. 3, pp. 368–378, 2016.

[19] T. Ishii and A. Masuda, "Annual degradation rates of recent crystalline silicon photovoltaic modules," *Prog. Photovolt.: Res. Appl.*, vol. 25, no. 12, pp. 953–967, 2017.

[20] C. R. Osterwald *et al.*, "Comparison of degradation rates of individual modules held at maximum power," in *Proc. 4th IEEE World Conf. Photovolt. Energy Conf.*, Waikoloa, HI, USA, 2006, vol. 2, pp. 2085–2088.

[21] R. Dubey *et al.*, "Comprehensive study of performance degradation of field-mounted photovoltaic modules in India," *Energy Sci. Eng.*, vol. 5, no. 1, pp. 51–64, 2017.

[22] J. Y. Ye, T. Reindl, A. G. Aberle, and T. M. Walsh, "Performance degradation of various PV module technologies in tropical Singapore," *IEEE J. Photovolt.*, vol. 4, no. 5, pp. 1288–1294, Sep. 2014.

[23] A. Ndiaye *et al.*, "Degradation evaluation of crystalline-silicon photovoltaic modules after a few operation years in a tropical environment," *Sol. Energy*, vol. 103, pp. 70–77, 2014.

[24] A. Limmanee *et al.*, "Degradation analysis of photovoltaic modules under tropical climatic conditions and its impacts on LCOE," *Renew. Energy*, vol. 102, pp. 199–204, 2017.

[25] M. C. Peel, B. L. Finlayson, and T. A. McMahon, "Updated world map of the Köppen-Geiger climate classification," *Hydrol. Earth Syst. Sci. Discussions*, vol. 4, no. 2, pp. 439–473, 2007.

[26] D. C. Jordan, C. Deline, S. R. Kurtz, G. M. Kimball, and M. Anderson, "Robust PV degradation methodology and application," *IEEE J. Photovolt.*, vol. 8, no. 2, pp. 525–531, Mar. 2018.

[27] PVLIB, Jan. 29, 2018. [Online]. Available: https://github.com/pvlib/pvlib-python

[28] D. C. Jordan and S. R. Kurtz, "The dark horse of evaluating long-term field performance—Data filtering," *IEEE J. Photovolt.*, vol. 4, no. 1, pp. 317–323, Jan. 2014.

[29] Y. Dazhi, P. Jirutitijaroen, and W. M. Walsh, "The estimation of clear sky global horizontal irradiance at the equator," *Energy Procedia*, vol. 25, pp. 141–148, 2012.

[30] R. M. Smith, D. C. Jordan, and S. R. Kurtz, "Outdoor PV module degradation of current-voltage parameters," in *Proc. World Renewable Energy Forum*, Denver, CO, USA, 2012, pp. 2547–2554.

[31] B. Marion *et al.*, "Validation of a photovoltaic module energy ratings procedure at NREL," Nat. Renew. Energy Lab., Golden, CO, USA, Rep. NREL/TP-520-26909, 1999.

[32] *Procedures for Temperature and Irradiance Corrections to Measured IV Characteristics of Crystalline Silicon Photovoltaic Devices*, IEC 60891, 2009.

[33] E. Hasselbrink *et al.*, "Validation of the PVLife model using 3 million module-years of live site data," in *Proc. 39th IEEE Photovolt. Spec. Conf.*, Tampa, FL, USA, 2013, pp. 7–12.

[34] D. C. Jordan, M. G. Deceglie, and S. R. Kurtz, "PV degradation methodology comparison—A basis for a standard," in *Proc. 43rd IEEE Photovolt. Spec. Conf.*, Portland, OR, USA, 2016, pp. 273–278.

[35] F. Pern, A. Czanderna, K. Emery, and R. Dhere, "Weathering degradation of EVA encapsulant and the effect of its yellowing on solar cell efficiency," in *Proc. 22nd IEEE Photovolt. Spec. Conf.*, Las Vegas, NV, USA, 1991, pp. 557–561.

[36] D. C. Miller *et al.*, "Degradation in PV encapsulation transmittance: An interlaboratory study towards a climate-specific test," in *Proc. 42nd IEEE Photovolt. Spec. Conf.*, New Orleans, LA, USA, 2015, pp. 1–6.

[37] C. Osterwald, A. Anderberg, S. Rummel, and L. Ottoson, "Degradation analysis of weathered crystalline-silicon PV modules," in *Proc. 29th IEEE Photovolt. Spec. Conf.*, New Orleans, LA, USA, 2002, pp. 1392–1395.

[38] Meteorological Service Singapore, Climate of Singapore, Jan. 29, 2018. [Online]. Available: http://www.weather.gov.sg/climate-climate-of-singapore/

[39] J. Lindroos and H. Savin, "Review of light-induced degradation in crystalline silicon solar cells," *Sol. Energy Mater. Sol. Cells*, vol. 147, pp. 115–126, 2016.

[40] D. C. Jordan *et al.*, "Silicon heterojunction system field performance," *IEEE J. Photovolt.*, vol. 8, no. 1, pp. 177–182, Jan. 2018.

Authors' photographs and biographies not available at the time of publication.